

Assessment of Osseointegration by Nonlinear Dynamic Response

Lance C. Ramp, DMD, PhD¹/Michael S. Reddy, DMD, DMSc²/Robert L. Jeffcoat, PhD³

Quantitative assessment of osseointegration remains a goal of researchers and clinicians alike. In this study, an instrument was designed for this purpose and tested in an animal model. Effective mechanical impedance, linearized for quasi-static force, was measured in 22 implants placed in the hind tibiae of 2 large hounds. The results demonstrate that in this animal long-bone model, the effective impedance of titanium root-form implants exhibits a degree of nonlinear behavior correlated with their state of osseointegration. This observation may be the basis for useful clinical instrumentation. (INT J ORAL MAXILLOFAC IMPLANTS 2000;15:197-208)

Key words: animal model, dental, histomorphometry, impedance, implant, mechanical, nonlinear, osseointegration

In this research, a noninvasive, nondestructive, and clinically applicable approach to the determination of implant osseointegration was investigated. The technique combines dynamic measurement of mechanical impedance with superimposed quasi-static loading, allowing the effective impedance of the (possibly) nonlinear implant system to be mapped as a function of applied load. While linear impedance components (eg, resonant frequency, damping ratio, and effective stiffness) may provide useful information about implant status, a detailed study of nonlinear impedance can yield additional insight into the bone-implant interface. Additionally, if these nonlinear data are expressed as ratios, they can be self-normalizing and therefore less subject to the variations in implant geometry, clinical technique, and other variables that complicate linear testing.

BACKGROUND

Brånemark demonstrated that an osseointegrated dental implant can provide a durable, functional, and predictable foundation for dental prostheses, provided that certain key criteria are met during surgery and subsequent treatment.¹ One of these requirements is that the implant be stable before loading. Since long-term studies indicate that most implant failures occur at implant exposure or within the first year of function,¹⁻³ an objective method of determining implant stability prior to loading is desirable.

According to Albrektsson, initial placement of the implant may result in 1 of 3 sequelae: interfacial bone may heal around the implant (osseointegrate), bone may remain as a necrotic sequestration, or a fibrous tissue interface may form.⁴ Over the longer term, the implant may fail from occlusal overloading or apical migration of bone. In the case of an osseointegrated implant, the bone and the implant surface are separated by a proteoglycan layer, whereas at failure, implants are commonly found to be encased in unstable soft tissue. For each case in which a non-bony layer exists at the bone-implant interface, there is the possibility of implant movement relative to bone,⁵ suggesting that a poorly integrated implant may show increased mobility through a limited range of motion. A nonlinear model of mobility is necessary to describe such changes in the bone-implant interface.

¹Assistant Professor, Department of Restorative Dentistry, University of Alabama School of Dentistry, Birmingham, Alabama.

²Professor, Department of Periodontics, University of Alabama School of Dentistry, Birmingham, Alabama.

³Research Professor, Department of Biomaterials, University of Alabama School of Dentistry, Birmingham, Alabama.

Reprint requests: Dr Lance C. Ramp, Department of Restorative Dentistry, University of Alabama School of Dentistry, 1919 7th Ave. S, Birmingham, Alabama 35294. Fax: 205-934-7901.

“Linearity” in the present context refers to a useful property of ideal structures; among other characteristics, each increment of applied load results in an equal increment of deflection in a linear system. This ideal behavior is only approximated in reality, since all real structures eventually stiffen, weaken, distort, or break as the load increases. The presence of nonlinear characteristics in the supporting structure of natural teeth was clearly demonstrated by Mühlemann,⁶ who observed that the incremental force required to displace a tooth a given distance increases markedly beyond an initial zone. (Viscoelastic behavior, also shown by Mühlemann, is not in itself a sign of nonlinearity.) An artificial implant surrounded by soft tissue would be expected to show similar nonlinear characteristics, although with substantially different property values resulting from its distinctive anatomy and support mechanism.

Mühlemann⁶ and others⁷⁻¹⁰ concentrated their attention on the linearized stiffness within the small-displacement zone, centered on the point of equilibrium between the tooth root and the periodontal ligament. By contrast, it is hypothesized that the nonlinear characteristics may themselves contain useful information about the state of implant osseointegration; specifically, that the effective stiffness varies significantly with moderate preload only if an implant is poorly integrated.

The method of mechanical impedance is commonly used to determine the stiffness, mass, and damping of dynamic systems. From these parameters, other quantities (such as resonant frequency and damping ratio) may be derived. The “bright ringing sound” characteristic of a successful implant reflects a combination of high resonant frequency and low damping ratio. Acoustic techniques, ranging from qualitative to elaborately instrumented, have been used in dentistry to measure the mobility of teeth^{11,12} and implants.¹³ Meredith et al¹⁴ recently employed resonant frequency alone to evaluate osseointegration in vivo.

The present study was designed to answer 2 questions: does the mechanical impedance of a well-integrated implant vary (ie, behave nonlinearly) in response to loading; and may linearized effective impedance, parameterized for loading, be used as a measure of osseointegration?

MATERIALS AND METHODS

To test these hypotheses, a purpose-built instrument was designed around a Brüel & Kjær (B&K, Naerum, Denmark) model 8001 impedance head, a load cell (Cooper Instruments, model LPM 530,

Warrenton, VA), and a battery-powered, hand-held shaker (B&K model 5691) (Figs 1a and 1b). The impedance head is equipped with a stiff 1.7-cm-long conical probe used to engage the implant. The shaker delivers a sinusoidal force induced by a programmable function generator (Hewlett-Packard model 33120A, Palo Alto, CA) and amplifier. The instrument was designed to produce a constant acceleration of approximately 2.5 m/sec². Custom analog circuitry provides continuous root mean square signal preprocessing for oscillatory force and acceleration prior to computer input. Data acquired with a data acquisition board (Data Translation, model DT 31-EZ, Marlboro, MA) are processed with a custom software program written in the DT-VEE 3.0 (Data Translation) environment. Velocity is derived from acceleration in closed form, and effective impedance \vec{Z} is calculated as the complex ratio \vec{F}/\vec{V} . The interested reader is referred to Hixson¹⁵ for a discussion of theoretical and practical aspects of impedance measurement.

Instrumentation Rationale

A brief discussion of the physical idea behind the instrument is required. “Preload” is the average force with which the probe tip is pressed laterally against the implant during measurement. While other researchers have generally taken care to minimize or control this loading,^{13,14,16,17} a randomly varying preload provides a straightforward way to stimulate and detect certain important types of nonlinear behavior. Applied by manual pressure, this preloading is called “quasi-static” because it varies much more slowly than the audio frequency oscillating force. If a compliant layer exists between the implant and the bone, it will be compressed on one side by the application of preload, giving rise (as hypothesized) to nonlinear effects.

One of the easiest type of nonlinearities to visualize, and one that frequently occurs in nature, is the stiffening spring sketched in Fig 2a. This model is qualitatively consistent with both Mühlemann’s⁶ measurements for natural teeth and the authors’ measurements on implants. In this example, additional springs come into play with increasing load, resulting in a nonlinear force-displacement curve (Fig 2b). The instrument superimposes small, rapid force oscillations on this preload and measures the differential stiffness, k_i (Fig 2c) at each preload (approximately the local slope of the force-displacement curve). The fact that Fig 2c is not a constant, horizontal line is sufficient to show that the system is not linear. This highly simplified example does not consider the fact that a real implant system will show smooth rather than abrupt property transitions and

will exhibit some degree of viscoelasticity. Such complications, however, are not essential to an understanding of the instrument.

There is an excellent practical reason to measure implant characteristics using dynamic methods rather than acquiring the static force-displacement curve directly. Provided that the frequency is high enough, the relatively massive head and jaw need not be immobilized to obtain accurate measurements. This approach captures both the static and dynamic (viscoelastic) characteristics of the implant.

Impedance is strictly defined only for linear systems, but in practice it is commonly applied to non-linear systems under specified conditions (usually, a limitation to small displacements). The term *effective impedance* makes explicit the fact that these assumptions are present and integral to the interpretation of the results. For this study, effective impedance is formally defined as the complex ratio of the fundamental small-amplitude oscillatory driving-point force and velocity vectors, parameterized on mean quasi-static preload force F_0 and oscillatory frequency ω :

$$\vec{Z}(\omega, F_0) = \vec{F} / \vec{V} \mid \text{preload } F_0, \\ \text{sinusoidal excitation at } \omega$$

This definition collapses to the ordinary definition of impedance when the system is linear.

Surgical Protocol

The surgical protocol was approved by the University Animal Use Committee, and all animal subjects were cared for in a humane manner. Figure 3 shows the sequence of events during the experiment. A total of 22 Steri-Oss implants (12 mm × 3.8 mm,



Fig 1a Photograph of experimental instrument.

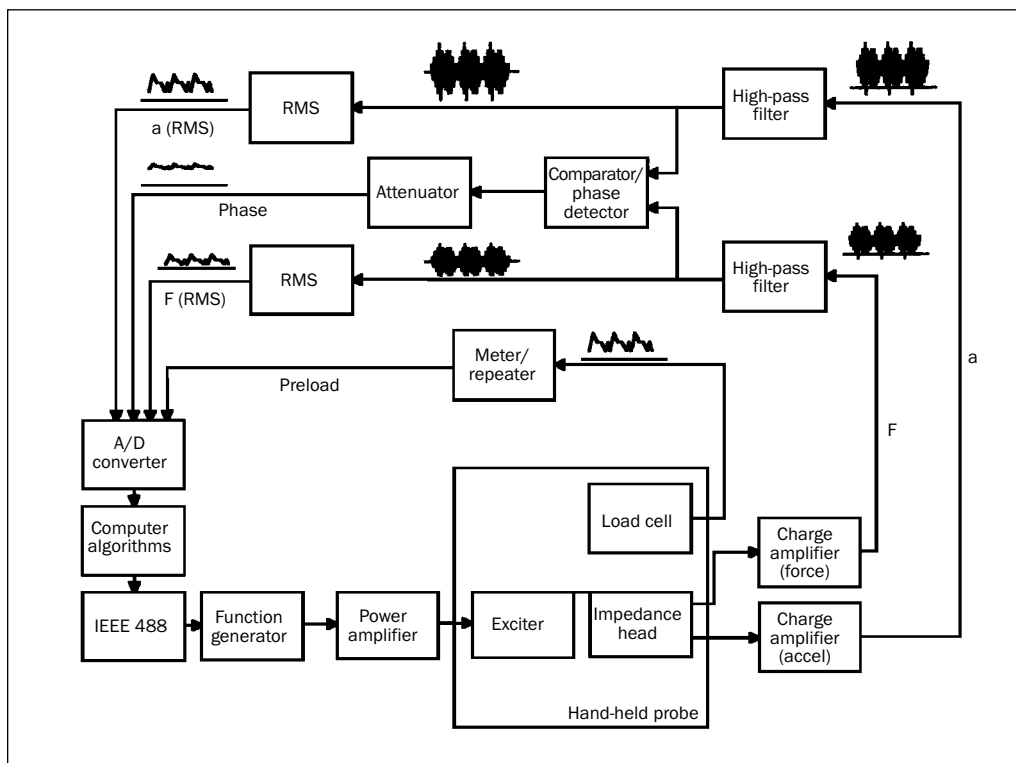


Fig 1b Block diagram of experimental circuitry.

threaded, hexlock, titanium root-form) (Steri-Oss Inc, subsequently Nobel Biocare, Yorba Linda, CA) was implanted into the hind tibiae of 2 Walker hounds. All surgical procedures were completed by a surgeon experienced in the placement of this dental implant system.

A combination of oxygen and isoflurane inhalation was used to induce and maintain each animal under general anesthesia. One g cephaloxin was administered intravenously. Standard operating room protocol for sterility was maintained at all times.

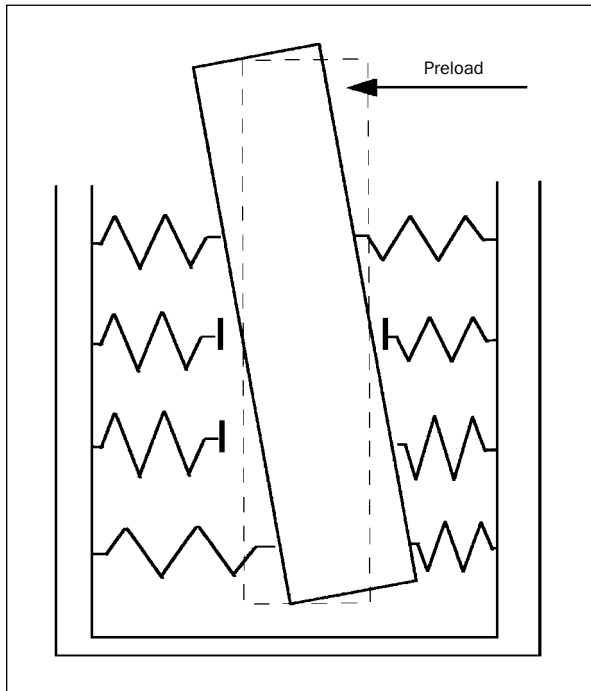


Fig 2a A simple nonlinear mechanical model with spring.

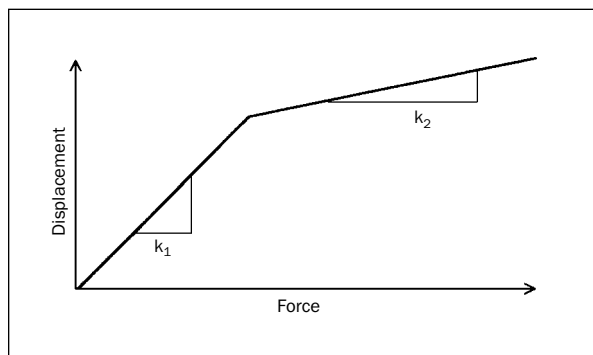


Fig 2b Force-displacement curve demonstrating the effect of preload in a nonlinear model.

Using a medial approach, an incision was made in the long axis of the right hind tibia, beginning approximately 1 cm below the stifle joint and proceeding inferiorly for a total length of approximately 6 cm.

The implant sites were prepared under continuous saline lavage with sequential enlargement of the crypt size. For this procedure, a Steri-Oss console (model 13555) was used with the accompanying handpiece. Drilling and counterboring speeds were each 1,800 rpm. Approximately 5 mm was allowed between implant sites. Threading of the implant site was performed at less than 50 rpm. Both animals received 5 implants optimally placed in the right hind tibia. During the recovery period, follow-up care was performed by the veterinary staff.

These implant sites were allowed to heal for 6 months. Recovery and wound healing were uneventful. At the end of 6 months, both animals were returned to surgery, and the previous implant sites were exposed. Three additional Steri-Oss implants were implanted in each animal distal to the implants placed earlier, using an identical technique except that the implant crypts were slightly oversized so that palpable movement of the implant was possible. These implants were then allowed to heal for 3 weeks.

Three weeks after the second surgery, the animals were again returned to surgery. Following a similar protocol, the animals were anesthetized and the implant site was uncovered. Three additional implants were optimally placed in the left hind tibia of each animal. All implants were exposed for examination at this time. Each implant was assigned an abutment assembly consisting of a 4-mm transmucosal abutment (Precision Margin Esthetics, Steri-Oss Inc) and cast gold healing cap to be used exclusively throughout testing. The difference in mass

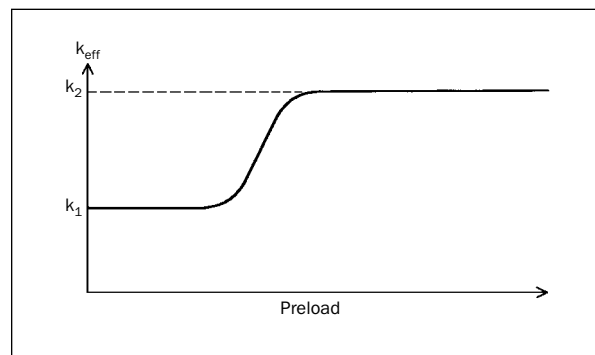


Fig 2c Effective stiffness versus preload in a nonlinear model.

among the abutment assemblies was less than 0.1 g. These abutment assemblies were attached to the implant with a 10 N-cm torque wrench.¹³ A small conical indentation on each gold cap was directed to face the operator, allowing him to engage the abutment assembly at a repeatable location, with the probe tip pointed normal to the long axis of the tibia.

Clinical and Laboratory Measurements

Each implant was first tested for clinical osseointegration by the conventional method of tapping with a metallic instrument (percussion testing) and examined for the presence of clinical mobility by pushing the implant back and forth between 2 blunt metallic instruments. Any implant with palpable mobility or dullness to percussion was classified as failed. There was no attempt to further classify clinical failures.

The experimental instrument was then used to characterize each implant. The probe tip was placed on the implant abutment so as to exert a preload normal to the long axis of the implant (Fig 4). The shaker was then actuated, and a measurement sequence was performed at 22 discrete frequencies, ranging from 100 to 4,150 Hz. Simultaneously, the operator randomly varied the preload placed on the implant by means of gentle hand manipulation of the instrument; preload was maintained between 0 and 2 N with the aid of an LED display on the end of the shaker. An elastic band kept the probe in contact with the implant at all times. Seventy-five sets of recorded oscillatory force (N), acceleration (m/sec^2), and preload (N) data triplets were acquired at each frequency for each implant.

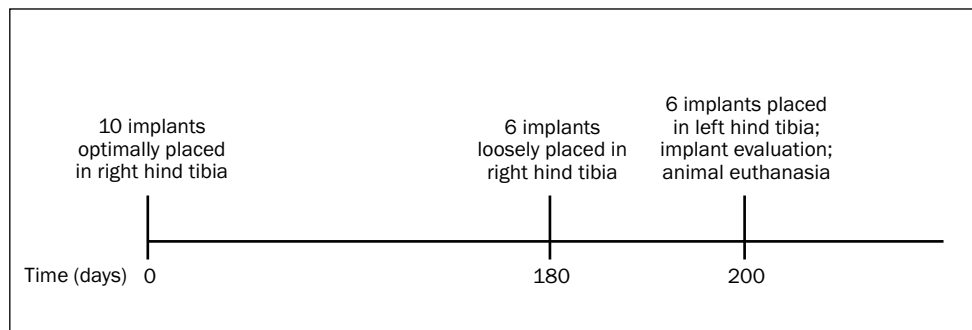


Fig 3 Schedule of experimental events.



Fig 4 Implants being tested with the instrument. The elastic band permits near-zero loading.

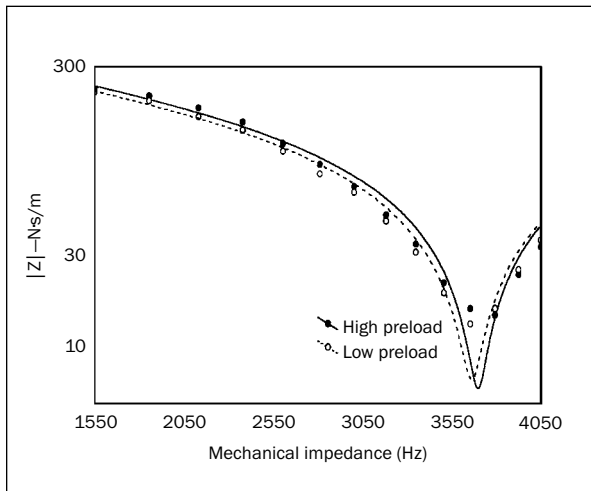


Fig 5a Effect of preload on mechanical impedance in a well-integrated implant.

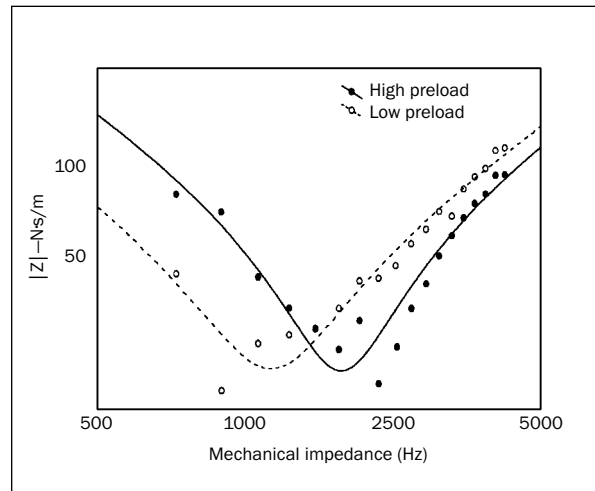


Fig 5b Effect of preload on mechanical impedance in a clinically failed implant.

Testing was performed on 3 categories of implants: 10 optimally placed implants in situ for 6 months; 6 implants in situ for 3 weeks (non-optimal placement, simulating initial failure to integrate); and 6 implants optimally placed (stable but nonintegrated) and tested just prior to euthanasia.

The animals were euthanized, and the retrieved tibiae were placed in PenFix (Richard-Allan Scientific, Kalamazoo, MI) for 48 hours. Each tibia was sectioned mediolaterally between each individual implant with a rotary disk and stored in 10% formalin solution. The specimens were dried in graded alcohol solutions and embedded in clear polymethyl methacrylate resin under vacuum. The embedded implants were hand-ground along the mediolateral plane of the tibia using custom brass jigs to obtain longitudinal sections at the 25% and 75% points along the implant diameter. Grinding was accomplished with successively finer silicon carbide grit paper and polished with 0.3- μm grit diamond slurry. The specimens were stained with van Gieson's solution (Polyscientific Research Corporation, Bay Shore, NY).

For all specimens, reflected light was used with high magnification (about 135 \times). The specimens were examined to quantify the total amount of bone at the interface using computerized histomorphometry with the Micro-Vu system and software (Micro-Vu Corporation, Windsor, CA). Because of anatomic differences among the tibiae, considerable variability was found in the amount and type of bone in contact with each implant. In some cases, bicortical attachment was noted; in others, only one cortical plate was engaged by the implant. For this

reason, histomorphometric measurement was limited to the total bone contact fraction.

The total perimeter of the implant section surface was measured by tracing a cursor around the visible edge of the implant, beginning and ending at the implant neck. The length of bone in apparent contact with the implant was then determined in a similar way. Finally, a ratio of bone in contact with the implant surface was determined. This procedure was carried out on all specimens using sagittal sections at 25% and 75% of the implant's outer diameter. The bone fraction used for data analysis represents the mean value obtained from these sections. The resolution of this technique does not permit measurement of proteoglycan thickness.

RESULTS

To capture the first-order effect of preload, each impedance datum was categorized based on preload into 2 arbitrary non-overlapping ranges ("low," 0 to 0.5 N, and "high," 1.0 to 2.0 N); intermediate preload values were excluded from the analysis. Mean effective impedance, effective stiffness (k_{eff}), natural frequency (ω_n), and damping ratio (ζ) were then computed as a function of frequency for each preload range. This sequence was carried out on each implant individually.

Figures 5a and 5b show representative impedance responses for osseointegrated and nonintegrated implants, respectively. For every implant tested, the impedance curve showed a distinct resonance peak and could be modeled satisfactorily as a

first-order system to determine ω_n , k_{eff} , and ζ . Variation in these parameters with preload is a measure of nonlinearity. Nonlinear behavior was expressed as 2 metrics: percent change in k_{eff} (Δk_{eff}), and percent change in ω_n ($\Delta\omega_n$) between the 2 preload groups. Experimental parameters were then plotted against bone fraction. Linear regression was used to determine a correlation coefficient for each curve.

Correlation with Histomorphometry

Figures 6 and 7 show the variation of selected dynamic parameters with bone fraction. Individual data for fresh, 3-week, and 6-month implants are shown, with derived regression lines overplotted; the correlation coefficient for each regression is shown with the figures. Table 1 summarizes the linear regression results for dynamic parameters versus bone fraction; the expected trend, based on first principles, is shown as a column in the table. Freshly placed implants are not included in the regression evaluations; their intimate contact with bone results from site preparation and insertion operations rather than healing or remodeling effects. They are shown for purposes of comparison.

Computed effective stiffness for all implants ranged from 0.2 to 3.5 MN/m. A positive correlation via linear regression was found between k_{eff} and bone fraction (Fig 6a). Damping ratio, ranging from 0 to 0.35, demonstrated a weak correlation with decreasing bone fraction (Fig 6b); the fact that all implants were underdamped suggests that viscoelasticity is not a good determinant of osseointegration. Positive correlation was also found with ω_n , which increases with bone fraction (Fig 6c). One of the 3-week implants underwent a significant amount of healing and registered a high resonant frequency, although the measured bone fraction demonstrated only 8.1% bone incorporation. With this exception, totally failed implants demonstrated generally lower resonant frequencies; however, the ability of resonant frequency alone to determine the bone fraction of a specific implant was not clear-cut.

Correlation of the nonlinear parameters Δk_{eff} and $\Delta\omega_n$ (Figs 7a and 7b) with bone fraction was less pronounced than the linear parameters. Although this correlation was not strong, it was consistent with expected trends in several categories.

Correlation with Clinical Measures

The correlation of instrument results with a clinical assessment of osseointegration was also of interest. For this study, clinical impression was recorded by a single examiner in 2 categories: sound on percussion (bright or dull) and perceptible mobility (yes or no). The raw data are reported in Table 2.

Of the 10 implants initially placed, none showed clinical evidence of failure. One of the 6 loosely placed 3-week implants registered as a clinical success. The bone around this implant was minimal and could reasonably be cast as a histologic failure. However, the healing process appeared to be well underway at the time of evaluation, and bone had to be removed to gain access to the implant.

In the case of gross clinical failure, the response of the instrument was unequivocal, as were the histologic evaluations. The failed implants were often more difficult to fit to a simple model because of their instability and the presence of higher-order effects, but even the simple model sufficed to quantify the large changes that occurred. Implants placed at euthanasia are also included in this evaluation because they met the limited clinical criteria to qualify as a success. Table 2 enumerates the findings of the clinical examination at the terminal appointment, including status of the implant and its response to percussion and mobility.

The statistical significance of each parameter in discriminating between the 2 clinical outcome groups was evaluated using 1-way analysis of variance (ANOVA). Clinical correlation with low-preload k_{eff} (Fig 8a) is distinctly apparent ($P < .00015$), as would be expected from the load-dependent nature of implant response and correlations noted with histomorphometry. A wide range of stiffness is seen in both high and low preload groups, but in general, lower k_{eff} was found to be associated with lack of osseointegration in this study. The association of ω_n with clinical outcome (Fig 8b) is also clear ($P < .00001$), though again there is some overlap between the clinically successful and clinically failed implants. A comparison of low-preload ζ with clinical findings (Fig 8c) shows a similar trend, with failed implants showing an increased ζ ($P < .00004$).

Although linear measures do reasonably well at classifying clinical osseointegration in a statistical sense, Figs 8a to 8c show considerable scatter within groups. This dispersion represents real physical variations in the implant-bone system, which may arise from various sources other than the state of integration. The motivation for using nonlinear metrics was to isolate the outcome of interest—osseointegration—from such extraneous factors a basic requirement for a practical clinical instrument. As Figs 9a and 9b demonstrate, this approach proved highly effective in distinguishing integrated from nonintegrated implants.

The nonlinear metrics $\Delta\omega_n$ and Δk_{eff} were compared to the dichotomous classification of clinical osseointegration. These quantities are defined such

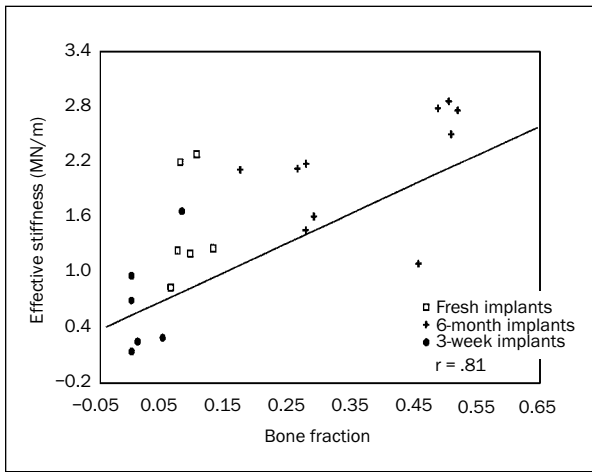


Fig 6a Low preload effective stiffness versus bone fraction ($r = .81$).

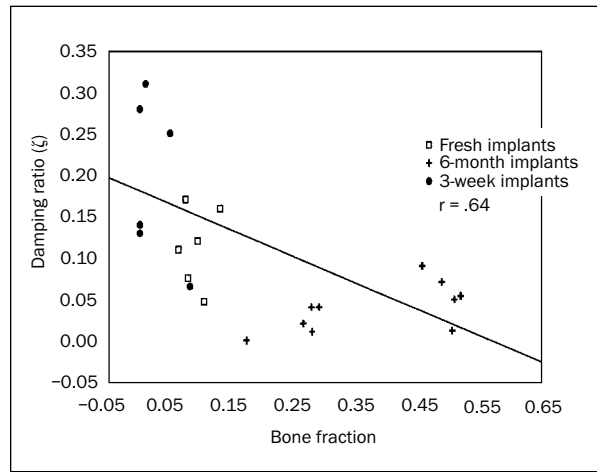


Fig 6b Low preload damping ratio versus bone fraction ($r = .64$).

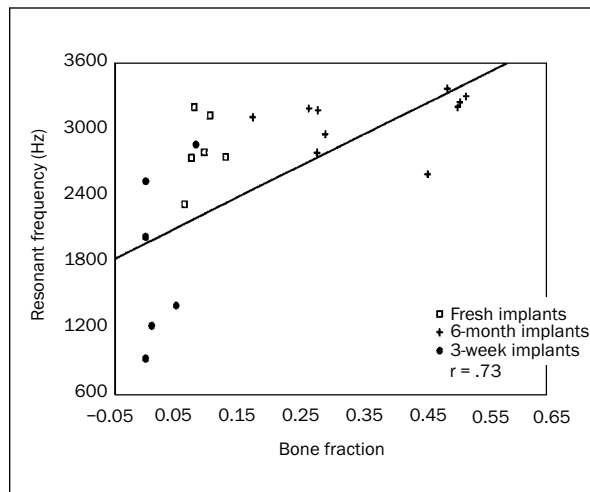


Fig 6c Low preload resonant frequency versus bone fraction ($r = .73$).

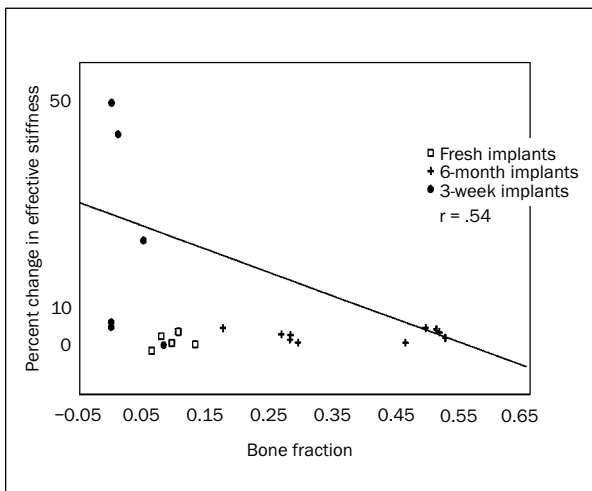


Fig 7a Percent change in effective stiffness versus bone fraction ($r = .54$).

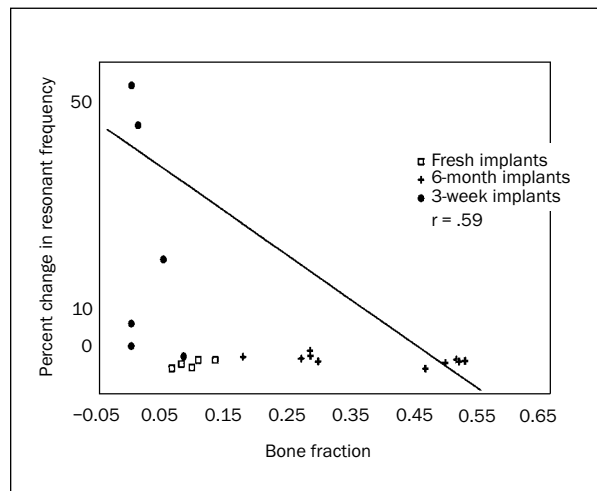


Fig 7b Percent change in resonant frequency versus bone fraction ($r = .59$).

Table 1 Summary of Parameter Response to Increasing Bone Fraction

Metric	Slope units	Expected slope	Slope	r
$k_{\text{eff high}}$	$\text{N}\cdot\text{m}^{-1}\cdot\text{percent}^{-1}$	+	$+3.7 \cdot 10^6$.81
$k_{\text{eff low}}$	$\text{N}\cdot\text{m}^{-1}\cdot\text{percent}^{-1}$	+	$+3.7 \cdot 10^6$.81
ζ	$\text{N}\cdot\text{s}\cdot\text{m}^{-1}\cdot\text{percent}^{-1}$	-	-0.31	.64
$\omega_n \text{ high}$	$\text{Hz}\cdot\text{percent}^{-1}$	+	+2297	.73
$\omega_n \text{ low}$	$\text{Hz}\cdot\text{percent}^{-1}$	+	+2840	.73
Δk_{eff}	percent^{-1}	-	-84.8	.56
$\Delta\omega_n$	percent^{-1}	-	-45.7	.54

Table 2 Clinical Impression and Status of All Implants

Dog/implant	Status	Percussion	Mobility	Class*
1				
1	6 months	Bright	No	I
2	6 months	Bright	No	I
3	6 months	Bright	No	I
4	6 months	Bright	No	I
5	6 months	Bright	No	I
6	3 weeks	Dull	Yes	NI
7	3 weeks	Dull	Yes	NI
8	3 weeks	Bright	No	I
9	1 hour	Bright	No	I
10	1 hour	Bright	No	I
11	1 hour	Bright	No	I
2				
1	6 months	Bright	No	I
2	6 months	Bright	No	I
3	6 months	Bright	No	I
4	6 months	Bright	No	I
5	6 months	Bright	No	I
6	3 weeks	Dull	Yes	NI
7	3 weeks	Dull	Yes	NI
8	3 weeks	Dull	No	NI
9	1 hour	Bright	No	I
10	1 hour	Bright	No	I
11	1 hour	Bright	No	I

*I = integrated; NI = nonintegrated, by clinical impression.

that a zero value corresponds to a linear system (ie, no change with static loading), and increasing values indicate an increasing degree of nonlinearity. In Fig 9a, it may be seen that the values of $\Delta\omega_n$ are clustered tightly around zero for the integrated implants, but widely dispersed (and as high as 50%) for nonintegrated implants. Figure 9b shows a comparable effect for Δk_{eff} . Both classifications are highly significant by 1-way ANOVA ($P < .00008$ for $\Delta\omega_n$ and $P = .00009$ for Δk_{eff}). More important, the radically different dispersion patterns between integrated and nonintegrated implants clearly indicate that the presence of this type of nonlinear response is diagnostic for osseointegration.

DISCUSSION

While no one parameter was entirely indicative of the status of the implant, all parameters investigated demonstrate trends consistent with expected behavior, suggesting the validity of the underlying model. For the nonintegrated category of implants, nonlinear metrics offered the most clear-cut delineation. Table 3 summarizes the parameters and the trends found in clinically failed implants. It should be understood that the determination of these nonlinear parameters depends on the preload category levels. In the absence of published precedents or other basis, the authors' load ranges were based on

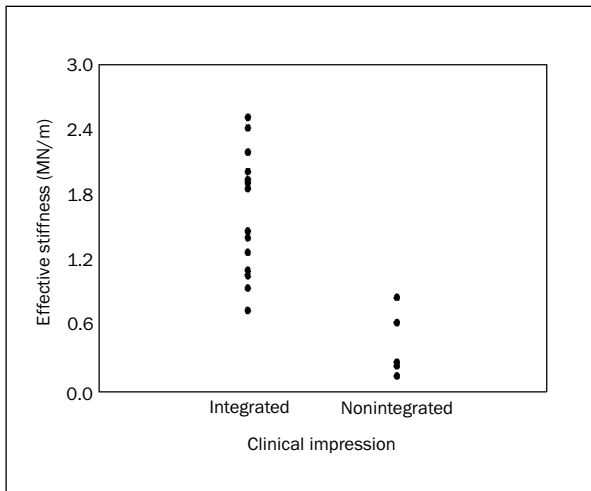


Fig 8a Low preload effective stiffness versus clinical impression ($P < .00015$).

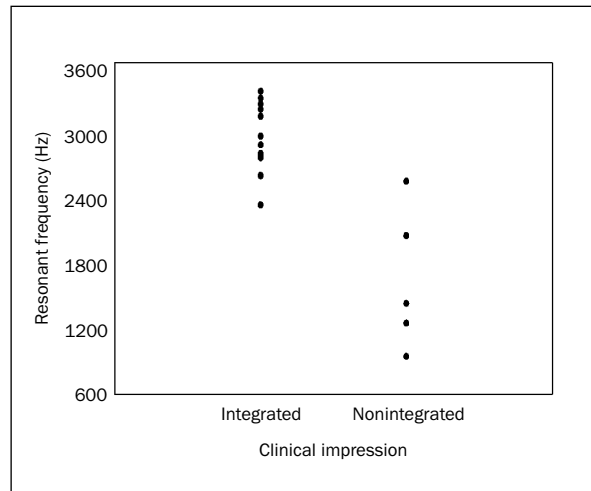


Fig 8b Low preload resonant frequency versus clinical impression ($P < .00001$).

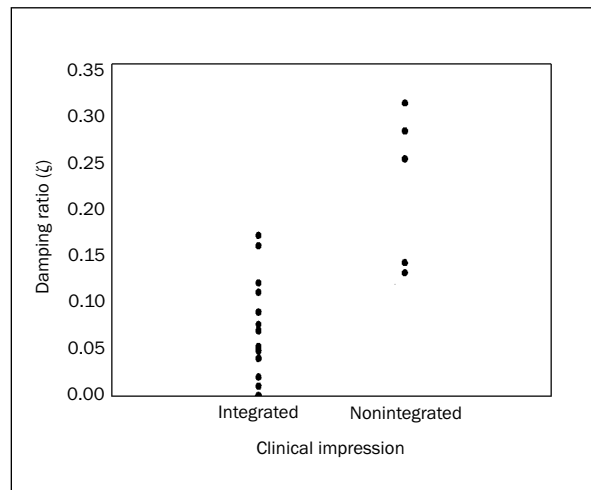


Fig 8c Low preload damping ratio versus clinical impression ($P < .00004$).

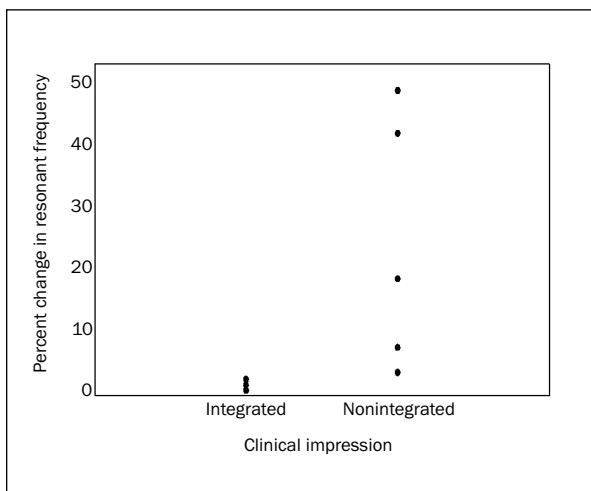


Fig 9a Percent change in resonant frequency versus clinical impression ($P < .00008$).

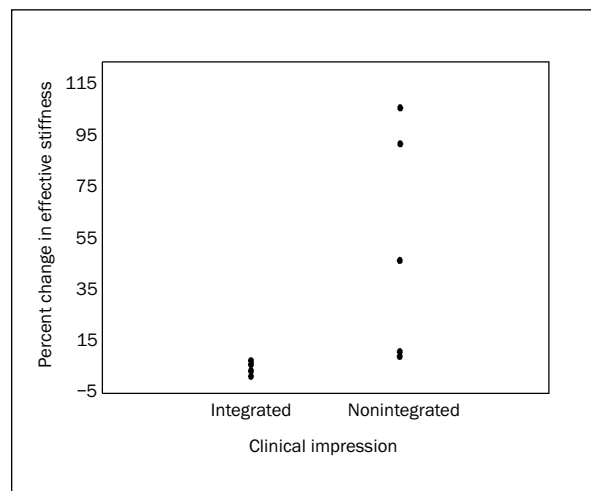


Fig 9b Percent change in effective stiffness versus clinical impression ($P < .00009$).

Table 3 Trends Associated with Clinically Failed Implants

Parameter	Trend found	Expected
k_{eff}	Lower	Yes
ω_n	Lower	Yes
ζ	Higher	Yes
$\Delta\omega_n$	Higher	Yes
Δk_{eff}	Higher	Yes

inspection of preliminary data. Other combinations of load ranges may demonstrate varying degrees of nonlinear behavior, and a continuous preload parameterization might be more appropriate.

Most of the resonant frequencies observed were found to be greater than 2 kHz, corresponding to a vibratory displacement amplitude of about 15 nm ($= 2.5 \text{ m/s}^2 / [2 \cdot \pi \cdot 2000]^2$). This small displacement is comfortably within the range given by other sources^{18,19} for the total thickness of proteoglycans and connective tissue layers in various states of osseointegration. One may reasonably conclude, therefore, that motions induced by the apparatus are consistent with the anatomic features of interest.

Since linear test results vary because of such factors as abutment length and implant type, these values cannot be readily compared to data obtained with other techniques. Meredith²⁰ correctly points out that quantification of the stiffness of the implant-tissue system is complicated by the stiffness of the implant components, stiffness of the bone at the interface, the anatomic features of the tissues engaged, and geometric factors of the implant. Using nonlinear parameters to evaluate osseointegration is appealing in part because the metrics, based on ratios, are to some extent self-normalizing and thus more nearly independent of extraneous variables.

In summary, evaluation of Δk_{eff} and $\Delta\omega_n$ between preload groups revealed a degree of nonlinear behavior in all categories of implants. This observation supports the idea that the bone-implant interface can be represented as a stiffening spring. The present research demonstrates that the mechanical impedance of endosseous dental implants, measured in an animal long-bone model, correlates with the state of osseointegration as determined by clinical findings and histomorphometry. Both linear and nonlinear metrics are influenced by the level of quasi-static loading parallel to the oscillatory excitation; this effect is apparent at the lowest levels of preload tested. The observed effects are generally consistent

with an implant-bone system that can be modeled as a mass constrained by a stiffening spring, along with relatively minor viscous damping. The frequency range and excitation amplitudes applied during the experiment were appropriate to excite motions of the implant within its supporting structures, a conclusion supported by known characteristics of osseointegrated implants.

CONCLUSION

This research provides 4 main findings that may be of value in future studies of osseointegration. First, it shows that the osseointegrated implant exhibits the nonlinear characteristics just described. Second, it indicates that the degree of nonlinearity is correlated with clinical implant stability over the range from integrated to nonintegrated. Third, it demonstrates, in the form of a manually preloaded exciter and impedance head, an experimental basis for clinically useful instrumentation for the objective evaluation of osseointegration. Finally, it provides a basis for following the progress of osseointegration over time using either linear or nonlinear impedance, particularly if a highly repeatable, noninvasive probe can be devised.

ACKNOWLEDGMENTS

This study was funded in part by NIDR grant K16DE00279. The authors gratefully acknowledge the additional support of Mr Don Kennard and Steri-Oss Inc (now Nobel Biocare) and the invaluable assistance of Dr Jack Lemons and Ms Martha Wilkins.

REFERENCES

1. Brånemark P-I, Adell R, Albrektsson T, Lekholm U, Lundkvist S, Rockler B. Osseointegrated titanium fixtures in the treatment of edentulousness. *Biomaterials* 1983;4:25-28.
2. Albrektsson T, Dahl E, Enbom L, Engevall S, Engquist B, Eriksson AR, et al. Osseointegrated oral implants. A Swedish multicenter study of 8139 consecutively inserted Nobel-pharma implants. *J Periodontol* 1988;59:287-295.
3. Jemt T, Chai J, Harnett J, Heath MR, Hutton JE, Johns RB, et al. A 5-year prospective multicenter follow-up report on overdentures supported by osseointegrated implants. *Int J Oral Maxillofac Implants* 1996;11:291-298.
4. Albrektsson T. Bone tissue response. In: Brånemark P-I, Zarb GA, Albrektsson T (eds). *Tissue-Integrated Prostheses: Osseointegration in Clinical Dentistry*. Chicago: Quintessence, 1985:129-143.
5. Chavez H, Ortman LF, DeFranco RL, Medige J. Assessment of oral implant mobility. *J Prosthet Dent* 1993;70:421-426.
6. Mühlemann HR. Periodontometry, a method for measuring tooth mobility. *Oral Surg Oral Med Oral Pathol* 1951;4:1220-1233.

7. Parfitt GJ. Measurement of the physiological mobility of individual teeth in an axial direction. *J Dent Res* 1960;39:608–616.
8. Körber KH. Electronic registration of tooth movement. *Int Dent J* 1971;21:466–477.
9. Persson R, Svensson A. Assessment of tooth mobility using small loads. *J Clin Periodontol* 1980;7:259–275.
10. D'Hoedt B, Lukas D, Mühlbrandt L, Scholz F, Schulte W, Quante F, Topkaya A. The Periotest—Research and clinical trials. *Dtsch Zahnärztl* 1985;40:113–125.
11. Noyes DH, Clark JW, Watson CE. Mechanical input impedance of human teeth in vivo. *Med Biolog Eng* 1968;6:487–492.
12. Oka H, Yamamoto T, Saratani K, Kawazoe T. Application of mechanical mobility of periodontal tissues to tooth mobility examination. *Med Biol Eng Comp* 1989;27:75–81.
13. Saratani K, Yoshida S, Oka H, Kawazoe T. The clinical measurement of the biomechanical mobility of dental implants. In: Kawahara H (ed). *Oral Implantology and Biomaterials*. Amsterdam: Elsevier, 1989:305–310.
14. Meredith N, Alleyne D, Cawley P. Quantitative determination of the stability of the implant-tissue interface using resonance frequency analysis. *Clin Oral Implants Res* 1996;7:261–267.
15. Hixson EL. Mechanical impedance and mobility. In: Harris CM, Crede CE (eds). *Shock and Vibration Handbook*. New York: McGraw-Hill, 1961:10.1–10.45.
16. Elias JJ, Brunski JB, Scarton HA. A dynamic modal testing technique for noninvasive assessment of bone-dental implant surfaces. *Int J Oral Maxillofac Implants* 1996;11:728–734.
17. Kaneko T, Nagai Y. Acoustoelectric technique for assessing the mechanical state of the dental implant-bone interface. *J Biomed Mater Res* 1986;20:169–176.
18. Albrektsson T, Brånemark P-I, Hansson H-A, Lindström J. Osseointegrated titanium implants. *Acta Orthop Scand* 1981;52:155–170.
19. Hansson H-A, Albrektsson T, Brånemark P-I. Structural aspects of the interface between tissue and titanium implants. *J Prosthet Dent* 1983;50:108–113.
20. Meredith N. Assessment of implant stability as a prognostic determinant. *Int J Prosthodont* 1998;11:491–501.